Journal of Urban and Environmental Engineering, v. 6, n. 1, p 01-09

ISSN 1982-3932
doi: 10.4090/juee.2011.v5n2.001009

Journal of Urban and Environmental Engineering

www.journal-uee.org

THE INTEGRATED WRF/URBAN MODELING SYSTEM AND ITS APPLICATION TO MONITORING URBAN HEAT ISLAND IN JAKARTA, INDONESIA

Laras Tursilowati[1,2*], Josaphat Tetuko Sri Sumantyo[1], Hiroaki Kuze[1] and Erna S. Adiningsih[2]

[1] *Center for Environmental Remote Sensing (CEReS), Chiba University, Chiba, 263-8522, Japan*
[2] *National Institute of Aeronautics and Space (LAPAN), Jl. dr. Junjunan 133, Bandung, 40173, Indonesia*

Received 15 June 2011; received in Revised form 15 November 2011 accepted 17 December 2011

Abstract: Population growth and urbanization will impact on city development through constructions of buildings, parking lots, streets, highways and driveways. These changes lead to the Urban Heat Island (UHI), which is an important factor for future urban planning. In this context, mesoscale climate models such as the Weather Research and Forecasting (WRF) model are useful for studying the potential deficit in open green areas. The analysis of remote sensing images can provide input data indispensable to such climate model studies. In this work, we analyze the land use/land cover information inside and around the city of Jakarta, Indonesia, to study how the land use (LU) change affects UHI that is characterized by the highest surface air temperature (*Ta*) of 306 K. It is found that LU modification with the addition of 25% urban area will expand the UHI area by around 43 km^2 (5%). On the contrary, with the addition of 58, 95 and 440% vegetation (grassland) in the urban area, the UHI area is reduced significantly, which are 255 km^2 (48%), 289 km^2 (54%) and 466 km² (88%), respectively. This indicates that the addition of more area with open green coverage results in more reduction of UHI area. The quantitative features of this relationship will be useful for urban planners to control the UHI effects that might degrade the living conditions in this megacity.

Keywords: Urbanization; urban heat island; weather research and forecasting

* Correspondence to: Laras Tursilowati. E-mail: laras@bdg.lapan.go.id.

INTRODUCTION

Urbanization is progressing rapidly in many Asian cities. The process of urbanization has modified the land use from the natural environment into the built environment (Maslin, 2004; Santamouris, 2006; Brauch *et al*., 2011). Climate change is projected to compound the pressures on natural resources and the environment, associated with rapid urbanization, industrialization and economic development (IPCC, 2007). Intensive urbanization can possibly lead to regional-scale climate change, called an Urban Heat Island (UHI) phenomenon (Santamouris, 2009).

The heat island is a reflection of the totality of microclimatic changes brought about by man-made alterations of the urban surface (Landsberg, 1981). Heat islands form in urban and suburban areas since many common construction materials absorb and retain more of the sun's heat than natural materials in less-developed rural areas (Gartland, 2008; Bolin, 2007). Combined effects of anthropogenic heating in city centers with those of low vegetation cover and dark surfaces can enhance the heat island effect (Taha, 1997). When surface temperature is high, the latent heat transport through evaporation becomes more effective for reducing temperature as compared with the upward flux of sensible heat (Saltzman, 1983). With little or no water to evaporate, the sunlight energy goes into raising the temperature of man-made structures such as roads and buildings. After sunset, the city is so warm that it never cools down as in the countryside around it, and so the heat island effect lasts all night long. Combining the effects of anthropogenic heating in city centers with those of other factors, such as the low vegetation cover and dark surfaces can enhance the heat island effect (Rapp, 2008; Taha, 1997).

The purpose of the present study is to investigate the influence of urban canopy structure on surface air temperature inside and around Jakarta based on spatially dense meteorological observations. Urban canopy parameterization with the help of numerical model studies is implemented, including the interaction between the meteorological field and urban canopy layer (UCL). Urban surface heterogeneities are essential factors that govern the UHI (Tursilowati *et al.*, 2009). Being the capital of Indonesia, the metropolis Jakarta is the largest city of the country, located on the northwest coast of Java island. The city area is at the mouth of the Ciliwung river that runs into the Jakarta Bay at an inlet to the Java Sea. Jakarta lies in a low, flat basin, averaging 7 m above sea level. In the northern city area, around 40% is below sea level, while the southern parts are comparatively hilly. The climate there is generally hot climate with maximum temperatures ranging from 32.7−34.0°C at noon, and minimum air temperature ranges from 23.8−25.4°C at night (DKI Jakarta provincial official portal, 2010).

In order to improve the understanding of processes that are related to neighborhood-scale climate and air quality, the UHI effects, and mesoscale circulation caused by urban-rural land cover differences, the use of mesoscale atmospheric models is increasing (Clarke *et al.*, 2005). Here we employ the Weather Research and Forecasting (WRF) model to simulate the UHI changes in relation to the land use (LU) changes, namely the changes in the land use type. The UHI effect, in turn, can be represented by the surface air temperature (T_a) at 2 m from the ground surface in the output of WRF model runs. The approach taken in this study will be useful for the prevention and control of UHI effects in association with future city planning and urban development.

WRF simulation

The WRF model is a mesoscale numerical weather prediction system designed to serve both operational forecasting and atmospheric research needs (WRF Model Website, 2010). The model has been designed to be a flexible simulation code that is efficient in a parallel computing environment. A modular single-source code is maintained that can be configured for both research and operations. It offers a large physical selection, so it is very useful in the modeling community (Skamarock *et al.*, 2008).

In this study, the WRF modeling system is applied to the Jakarta metropolitan areas to evaluate the influence of urban-scale surface coverage to UHI effects, based on observation in the year 2002. Here we use the Python/Delphi platform to incorporate the modification of the LU types in our urban modeling system. The Delphi programming language is an extension of the Pascal language that was designed for use in the object-oriented programming arena, called Object Pascal. Python program is part of a growing open-source software community, which includes the Linux operating system, the Perl scripting language, the Apache Web server and numerous other projects (Abolrous, 2000; Deitel *et al*., 2002; Pilgrim, 2004). Such an approach is considered to be very valuable for urban planners to design the city environment friendly to the residents.

DATA AND METHODOLOGY

NCEP FNL data

National Centers for Environmental Prediction (NCEP) Final (FNL) Operational Global Analysis data provide surface pressure, sea level pressure, geopotential height, temperature, sea surface temperature, soil values, ice cover, relative humidity, u- and v- winds, vertical motion, vorticity and ozone on 1.0 × 1.0 degree grids continuously at every six hours (UCAR, 2010). This

is operationally run four times a day in near-real time at NCEP. The analyses are available at 26 mandatory (and other pressure) levels from 1000 mb to 10 mb, including the surface boundary layer and some sigma layers. Time period employed in this study is from 2 to 4 February 2008, with the benchmark of FNL data (fnl_080202_00_00–fnl_080204_00_00) in six hour time steps.

Land use data

A global land use/land cover (LULC) database classified according to the United States Geological Survey (USGS) LULC system is provided with WRF. In this work, the WRF model was set up by using four nests at 27, 9, 3 and 1 km horizontal grid spacing for domain 1, 2, 3 and 4, respectively (**Fig. 2**). Since the extent of the Jakarta metropolitan area is underpresented in the USGS dataset, we also use a more recent land cover classification for the Jakarta metropolitan region, base on the 2003 IKONOS-satellite with resolution 1 m panchromatic and 4 m multispectral (Tursilowati *et al.*, 2009). This detailed classification result is incorporated into WRF by re-projecting the regional land cover map onto the USGS dataset using standard GIS and remote sensing using supervised classification methods. Each WRF 30-s grid cell is assigned with the land cover class with the highest fraction coverage (Tursilowati *et al.*, 2009). This land cover data is used as the original LU (LU origin) input to the WRF Model.

Observational data

The three stations observational data used in this study are the air temperature data from meteorological stations operated by the Buerau of Meteorology, Climatology and Geophysics. Locations of observation data are Tanjung Priok (6^{0}06’ S, 106°52’ E), Observatorium-Jakarta (6°10’ S, 106°49’ E) and Soekarno Hatta (6°07’S, 106°39’ E). The period data from 2 to 4 February 2008 are used, in synchronization with the time period of model runs.

PC Cluster Specification

The PC cluster used in this study (**Fig. 1**) is similar to the system described in a reference (Wang *et al.*, 2007). The major features of our system are as follows.

1-Server: Dual core processor (AMD) with motherboard memory of 4112232 kB and SATA 300 GB hard disk, operated by Linux OS 5 (Redhat Enterprise).

2-Node clusters: 15 node clusters, with each node having dual core processor (AMD1211), SATA Raid, DDR2 20597884 kB, and 500 GB HDD, operated by Linux OS 5.

Fig. 1 PC cluster built at the National Institute of Aeronautics and Space (LAPAN), Bandung.

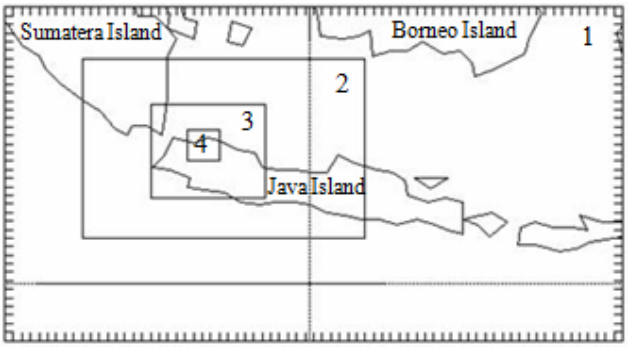

Fig. 2 Plot the nesting of four regions 1, 2, 3 and 4.

3-Softwares: Redhat Linux 5, Advance Research WRF Version 3 (AR-WRF V3), Fortran 90 Compiler, Grids Analysis Display System (GrADS), NetCDF, HDF4, Matlab, Vis5D, MPICH2 (PGI+GCC), Apache, Php and MySQL.

Domain configuration

The domain configuration used in the WRF model calculation is shown in **Table 1**. This configuration is basically the same as the one described in literatures (Wang *et al.*, 2007; UCAR, 2010).

Figure 2 shows the nesting of four regions used for running the model, namely the first (widest) nesting with the area of 1°23’–10°16’S, 100°44’–118°33’E (western Indonesia), the second one with 3°40’–8°27’S, 103°02–111°26’E (Java and southern Sumatera), the

Table 1. The domain configuration in the WRF model

Field	Domain 1	Domain 2	Domain 3	Domain 4
Meridional Grid Dimension	73	100	121	100
Zonal Grid Dimenssions	40	64	100	100
Vertical Level	31	31	31	31
Grid Resolution	27 km	9 km	3 km	1 km
Terrain Resolution	10 min (~18 km)	5 min (~9 km)	2 min (~4 km)	30 s (~0.9 km)
Explicit Moisture Scheme	WRF SM 3–class scheme	WRF SM 3–class scheme	Purdue Lin scheme	No micro-physics
Longwave Radiation Scheme	RRTM scheme	RRTM scheme	RRTM scheme	RRTM scheme
Shortwave Radiation Scheme	Dhudia scheme	Dhudia scheme	Dhudia scheme	Dhudia scheme
Surface Layer	MM5 similarity	MM5 similarity	MM5 similarity	MM5 similarity
Land Surface Physics	5-layer thermal diffusion	5-layer thermal diffusion	5-layer thermal diffusion	5-layer thermal diffusion
Cumulus Scheme	Betts-Miller-Janjic scheme	Betts-Miller-Janjic scheme	Kain-Fritsch scheme	No cumulus scheme
PBL Type	YSU scheme	YSU scheme	YSU scheme	YSU scheme

*SM=Single Moment, RRTM=Rapid Radiative Transfer Model, MM5=Mesoscale Model5, YSU=Yonsei University

third one with 5°14'–7°32'S, 105°19'–108°33'E (West Java), and the fourth one with 5°20'–6°25'S, 106°30'–107°12'E (Jakarta and its surrounding area). For each of the first to fourth domain configurations, the spatial resolutions are 27, 9, 3 and 1 km, respectively.

Land use modification

In the model run, hypothetical modification of LU is implemented in accordance with the following four scenarios: (s1) modification of all the grassland into urban type (reducing 100% grassland), (s2) modification by added 48% of grassland (s3) added 95% grassland, and (s4) added 440% grassland. The open-source programs of Delphi/Python are used to modify the LU type. In (s1), Delphi program modifies all of grassland area into urban area: in terms of the USGS standard change from index 7 to index 1, whereas Python program is used to modify the LU by adding the land use type per grid manually (s2–s4).

Parameterization of longwave radiation balance, anthropogenic heat flux and heat storage

The sky-view factor is a dimensionless parameter between 0 and 1, representing the fraction of visible sky at a reference site in comparison with the sky fraction over a flat horizontal surface without view obstruction (Clarke *et al.*, 2005). The sky-view factor for a road of an infinitely long urban canyon is calculated as a function of the road width w (m) and the building height. The assumption of infinitely long urban canyons can be justified because of the grid structure of roads and the housing density in the suburban developments of Jakarta. The sky-view factor is introduced to the longwave radiation balance R_{long} (Wm^{-2}) of the urban land cover categories in the WRF slab model (Dudhia, 1993).

Numerical design

The nesting simulations are conducted for the original (unmodified) LU and four LU use modifications (s1–s4) using the four horizontal domains. The overall scheme of the methodology is shown in **Fig. 3**.

RESULTS AND DISCUSSION

Land use modification

Different LU distribution data are used as input data to the WRF model runs. The original LU map in and around Jakarta (5°20'–6°25' S, 106°30'–107°12' E) is shown in **Fig. 4**.

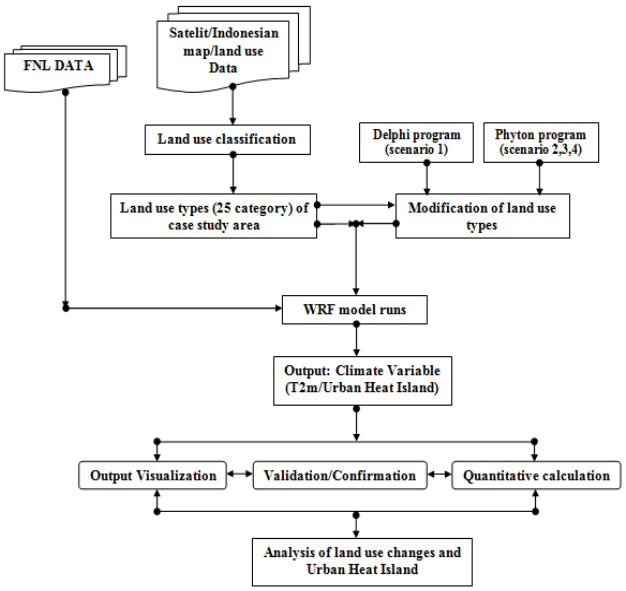

The legend indicates the LU index taken from the USGS standard categories (see **Table 2**). As seen from **Fig. 4**, the LU distribution consists of 10 types, namely, (LU index 1) urban, (2) dryland cropland/pasture, (3) irrigation cropland/pasture, (5) cropland/grassland mosaic, (7) grassland, (8) shrubland, (16) waterbody, (17) herbaceous wetland, and (19) barren/sparse vegetation. Among these, dominant LU types in Jakarta are (1) urban, (3) irrigation cropland/pasture, and (16) waterbodies including the ocean in the northern part. The urban area is concentrated in the central part of the study area shown in **Fig. 4**. Moderately found categories are (2) dryland cropland/pasture, (5) cropland/grassland mosaic, and (7) grassland.

Figure 5 represents the result of LU modification according to (s1), in which all the grassland has been changed into urban. **Figure 6** shows the result of LU modification from the original LU using the (s2) to (s4), with the change from urban to grassland with a fraction of around 58% (s2) (**a**), 95% (s3) (**b**), and 440% (s4) (**c**).

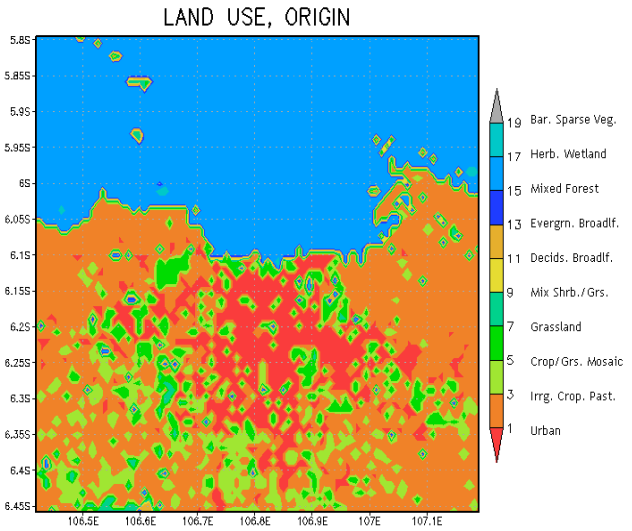

Fig. 4 Original (unmodified) land use.

Table 2. Land use index of USGS categories

LU Index	Description LU type	LU Index	Description LU type
1	Urban	13	Evergrn. Broadlf.
2	Dryland Crop Past.	14	Evergrn. Needlf
3	Irrg. Crop. Past.	15	Mixed Forest
4	Mix. Dry/Irrg.C.P.	16	Water Bodies
5	Crop./Grs. Mosaic	17	Herb. Wetland
6	Crop./Wood Mosc	18	Wooded wetland
7	Grassland	19	Bar. Sparse Veg.
8	Shrubland	20	Herb. Tundra
9	Mix Shrb./Grs.	21	Wooden Tundra
10	Savanna	22	Mixed Tundra
11	Decids. Broadlf.	23	Bare Gmd. Tundra
12	Decids. Needlf.	24	Snow or Ice

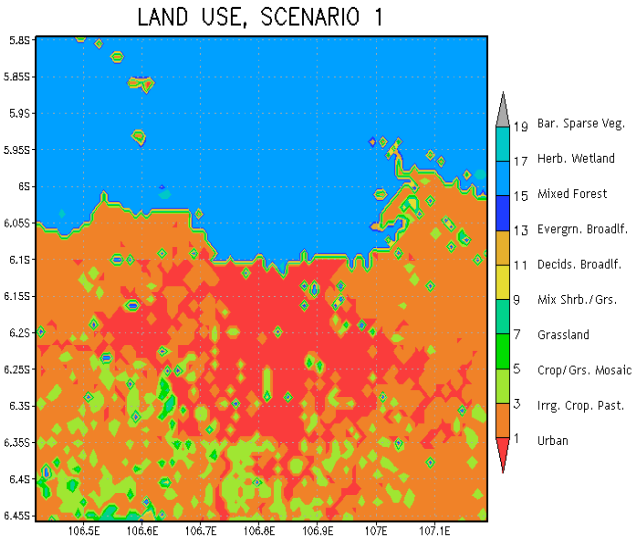

Fig. 5 Land use modification resulting from s1 (grassland is modified to urban: LU index change of 7 to 1).

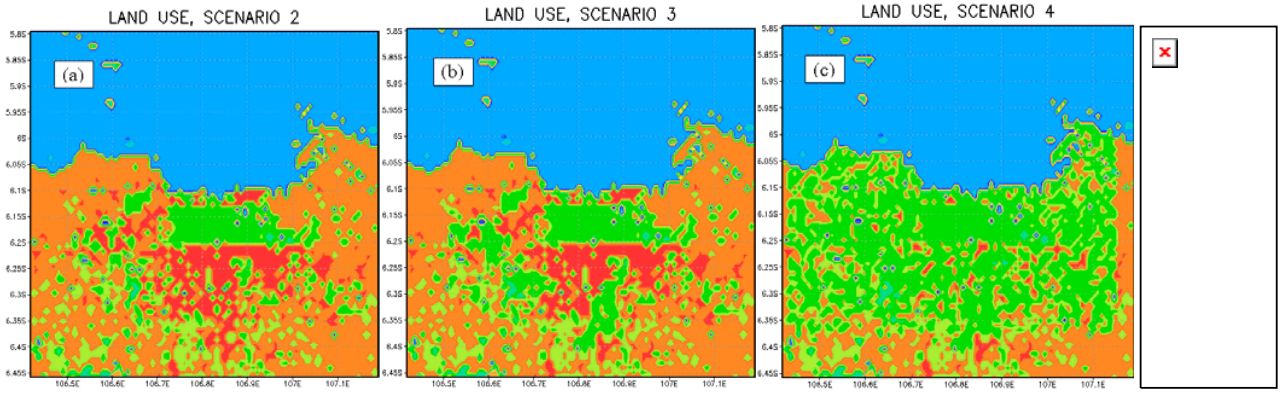

Fig. 6. Land use modification by changing a fraction of urban area into grassland: (a) 58% (s2), (b) 95% (s3) and (c) 440% (s4).

The statistics of LU before (LU origin) and after modification is shown in **Fig. 7**. It is noted that the categories of dryland/cropland and pasture (index 2), cropland/greenland mosaic (index 5), and waterbodies (index 16) are unchanged in all the scenarios, whereas those of urban (index 1), irrigation cropland/pasture (index 3), and grassland (index 7) has been changed.

Figure 8, on the other hand, shows the land area that has been changed as compared to the original distribution. The fractional changes are summarized in **Table 3**. By reducing 100% grassland, the urban area increased to 339 km^2 (from 1360 to 1699 km^2). With the addition around 58, 95 and 440% grassland, then the urban area was reduced 185 km^2 from origin (±14%), 309 km^2 (±23%) and 835 km^2 (±61%), respectively (**Table 3**).

Urban Heat Island

The distributions of T_a obtained from the WRF model calculations are shown in **Fig. 9** (spatially) and statistically shown by **Figs 10–11** and **Table 4**. All the panels shown in **Fig. 9** are from WRF model runs at a time step corresponding to around 11:00 a.m. local time.

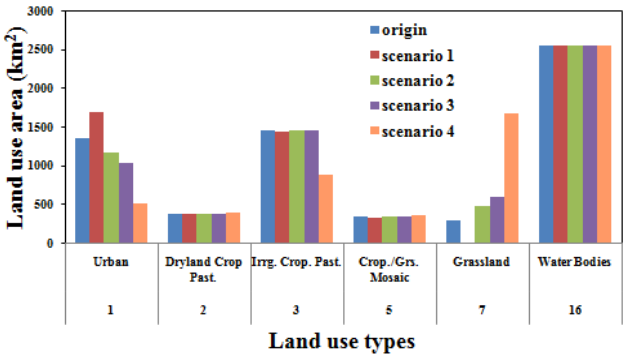

Fig. 7 Graphs of land use (origin and after modification) (km^2) as input for WRF model runs.

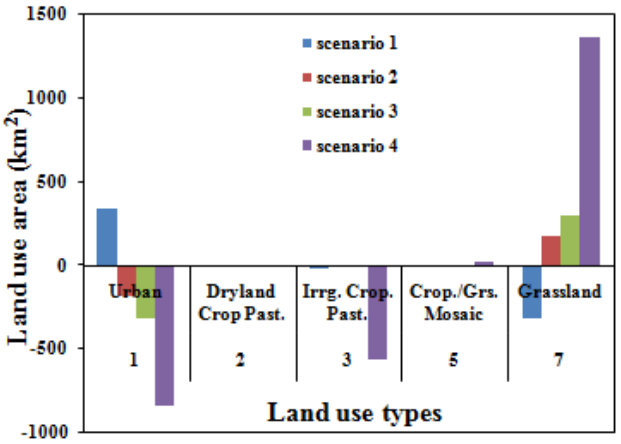

Fig. 8 The changes of LU before and after modification (km^2).

Table 3. Fractional changes from the original LU

LU Index	Land Use Types	scenario 1	scenario 2	scenario 3	scenario 4
1	Urban	25%	-14%	-23%	-61%
2	Dryland Crop P.	-2%	0%	1%	2%
3	Irrg. Crop. Past.	-1%	0%	0%	-39%
5	Crop./Grs. Mos.	-1%	0%	1%	6%
7	Grassland	-100%	58%	95%	440%

The T_a obtained with the original LU is shown in **Fig. 9a**. As seen in this figure, the pattern of UHI is concentrated in urban areas with T_a about 306 K (red color), while the surrounding area having the LU of a mixture of dry land, rice paddies, and irrigation shows a lower T_a. **Fig. 9b** (s1) shows the spread of UHI area by approximately 43 km^2 (5%) with the addition of 25% urban (i.e., reduction of 100% grassland). Thus, it can be confirmed that the UHI occurs in the central city. The influence of including more vegetation area, on the other hand, can be seen from **Figs 9c–e**. In **Fig. 9c** (s2) the UHI area characterized with T_a 306 K decreases by approximately 48% (255 km^2) when 58% of grassland added. In **Fig. 9d** (s3) the UHI decreases by approximately 54% (289 km^2) with the addition of 95% grassland, while **Fig. 9e** (s4) shows the reduction of approximately 88% (466 km^2) with the addition of 440% grassland. Especially in **Fig. 9e**, it is seen that the distribution of the highest T_a appears in the very limited region. This is due to the addition of a wide spread of grassland, around 440%. **Figure 11** shows the changes of area distributions in accordance with T_a ranges after the LU modification.

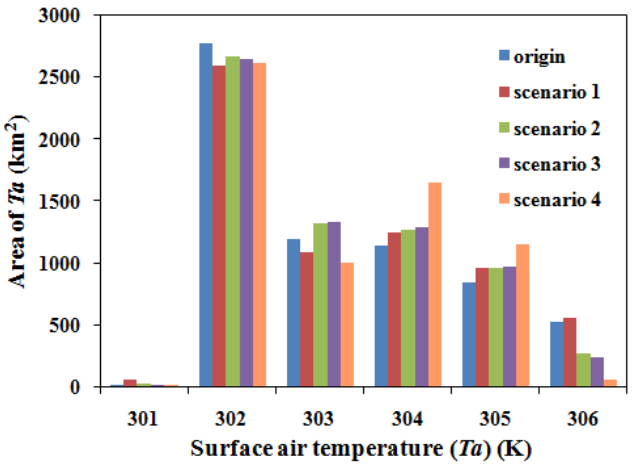

Fig. 10 Distributions of T_a from the results of WRF model runs.

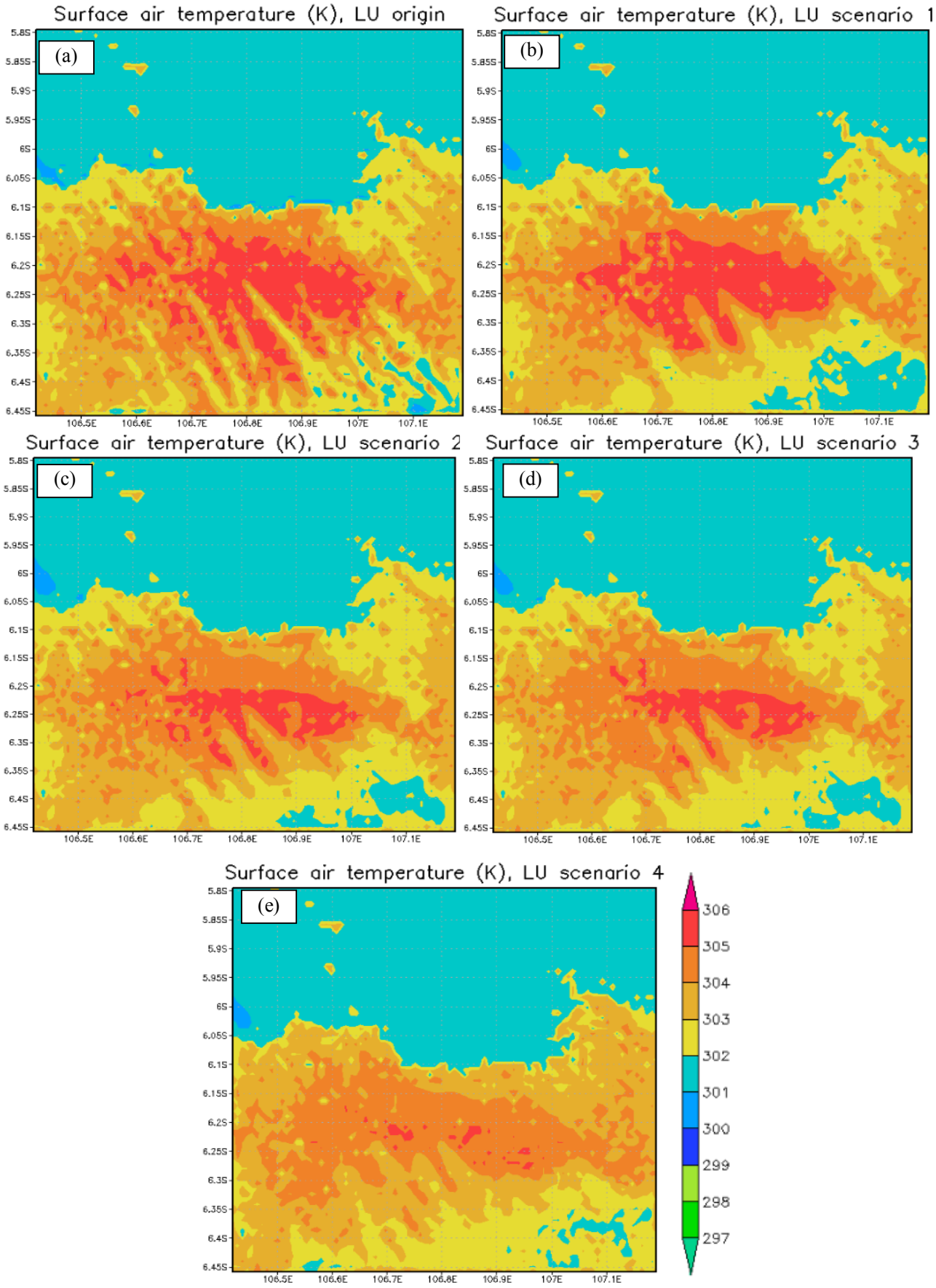

Fig. 9 T_2 (K) from WRF runs with input (a) LU origin, (b) LU index 7 to 1, (c) +58%, (d) +95%, and (e) +440% grassland

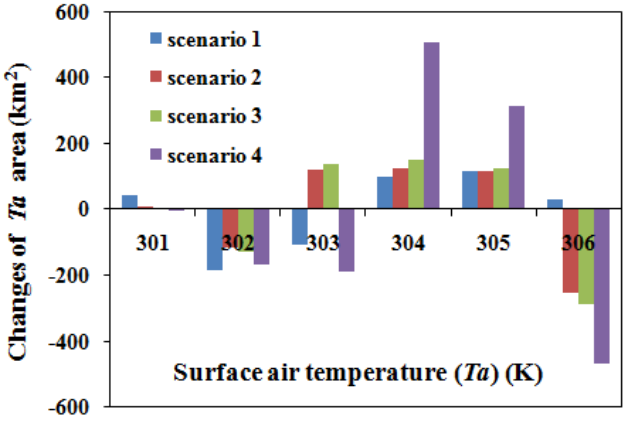

Fig. 11 The changes of T_a area after land use modification

Model Validation

T_a as one of the variable's output from WRF model runs (using LU origin as input) have validated by observation data from The Agency of Meteorology, Climatology and Geophysic (BMKG) Indonesia to confirm the accuracy of our methodology. Locations of observation data are Tanjung Priok (6°06'S, 106°52'E), Observatorium-Jakarta (6°10'S, 106°49'E) and Soekarno Hatta (6°07'S, 106°39'E). The result of model validation is shown in **Fig. 12**.

The range of R-squared value (R^2) T_a WRF model runs compare an observation data as the reliability value between 0.499–0.641 (**Fig. 12**). This represents the strong correlation (Ott & Longnecker, 2001; Pallant, 2007). Validation of model runs with observation data shows WRF model is good enough to represent the actual climate conditions (T_a).

CONCLUSIONS AND FUTURE WORKS

The analysis of the land use (LU) change affects the Urban Heat Island (UHI) inside and around Jakarta city as the capital of Indonesia using the Weather Research and Forecasting (WRF) has been studied. The LU modification using Delphi and Python program have applied to investigate UHI spreading. UHI characterized by highest surface air temperature (T_a) of 306 K. The spatial and graphical analysis shows significant differences. LU modification of grassland into urban area will expand the area of UHI around 43 km^2 (5%).

Table 4. Changes of T_a area from origin in percentage

T_a (K)	scenario 1	scenario 2	scenario 3	scenario 4
301	226%	47%	16%	5%
302	-7%	-4%	-5%	-6%
303	-9%	10%	11%	-16%
304	9%	11%	13%	44%
305	14%	14%	15%	37%
306	5%	-48%	-54%	-88%

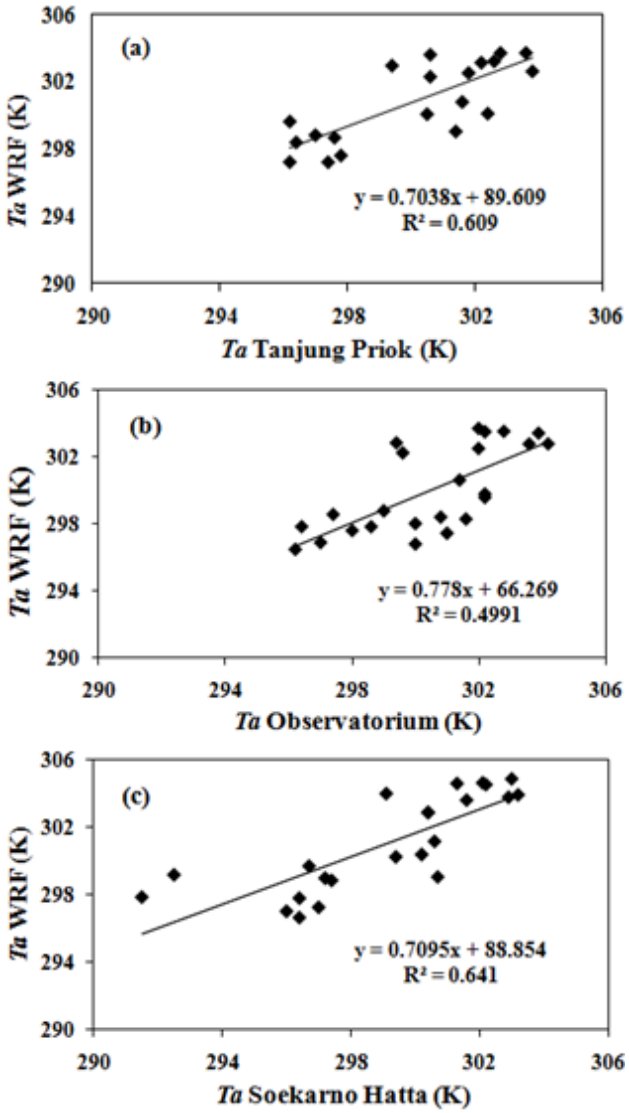

Fig. 12 T_a Validation of WRF model runs with observation data (a) Tanjung Priok, (b) Observatorium and (c) Soekarno Hatta.

In contrary, the addition of grassland would reduce the UHI. By adding more vegetation, there will be more areas of high temperature, which dropped the temperature. Quantitatively with the addition 48, 95 and 440% vegetation (grassland) in urban area, the UHI (306 K) area is reduced 48, 54 and 88% respectively. The model accuracy is the strong correlation with the observation data (R^2 around 0.499–0.641). This study can be used as reference for good urban design and comfortable environment.

The results of this study can still be developed by modification of land use by changing the other land use type, so that the results of running the model will be analyzed further for the sake of a better city planning. The future work is to analyze the other climate variables (i.e. albedo, latent heat flux, planetary boundary layer height, accumulated total precipitation cumulus, etc.).

Acknowledgment The authors wish to thank to the Japan Society and Promotions Science (JSPS) Ronpaku program and National Institute of Aeronautics & Space (LAPAN, Indonesia) for the funding of this research conducted at the Center for Environmental Remote Sensing (CEReS), Chiba University, Japan and Center for Atmospheric Sciences & Climate Application, LAPAN-Bandung, Indonesia.

REFERENCES

Abolrous, S.A. (2000) *Learn Pascal*. Wordsare Publishing, Inc. Plano, Texas.

Bolin, B. (2007) *A History of The Science and Politics of Climate Change: The Role of the Intergovernmental Panel on Climate Change*. Cambridge University Press, Cambridge, United Kingdom.

Brauch, H.G., Spring, U.O., Mesjasz, C., Grin, J., Mbote, P.K., Churou, B., Dunay, P. & Birkmann, J. (2011) *Coping with Global Environmental Change, Disasters and Security: Threats, Challenges, Vulnerabilities and Risks*. Springer, Berlin Heidelberg.

Clarke, S.G., Zehnder, J.A., Stefanov, W.L., Liu, Y. & Zoldak, M.A. (2005) Urban Modifications in a Mesoscale Meteorological Model and the Effects Near-Surface Variables in an Arid Metropolitan Region, *J. Applied Meteorol.* **44**(9), 1281–1297. doi: 10.1175/JAM2286.1

Deitel, H.M., Deitel, P.J., Liperi, J.P. & Wiederman, B. (2002) *Python How to Program*. Prentice Hall.

DKI Jakarta Provincial Official Portal (2010) Available in: http://www.jakarta.go.id. accessed in 20 September 2010.

Dudhia, J. (1993) A nonhydrostatic version of the Penn State–NCAR Mesoscale Model: Validation tests and simulation of an Atlantic cyclone and cold front. *Mon. Wea. Rev.* **121**, 1493–1513.

Gartland, L. (2008) *Heat Islands: Understanding and Mitigating Heat in Urban Area.*, Earthscan, London-Sterling.

IPCC (2007) Intergovernmental Panel on Climate Change, Fourth Assesment Report, Climate Change 2007: Synthesis Report.

Landsberg, H.E. (1981) *The urban climate*. Academic Press, London.

Maslin, M. (2004) *Global warming: a very short introduction*. Oxford University Press, Oxford, New York.

Ott, R..L. & Longnecker, M. (2001) *An Introduction to Statistical Methods and Data Analysis*, Duxbury, Thomson Learning, USA.

Pallant, J. (2007) *SPSS Survival Manual: A step by step guide to data analysis using SPSS for Windows*, third edition, Mc Graw Hill, Open University Press, New York, USA.

Pilgrim, M. (2004) *Dive into Python*. Apress, Python Software Foundation.

Rapp, D. (2008) *Assessing Climate Change: Temperatures, Solar Radiation and Heat Balance*. Springer, California-USA.

Saltzman, B. (1983) *Theory of Climate, Advances in Geophysic, vol. 25*. Academic Press, New York, London.

Santamouris, M. (2006) *Environmental Design of Urban Building: An Integrated Approach*. Earthscan, London-Sterling.

Santamouris, M. (2009) *Advances in Building Energy Research, (ABER)* Earthscan, London-Streling, VA.

Skamarock, W.C., Klemp, J.B., Dudhia, J., Gill, D.M., Barker, D.O., Wang, W. & Powers, J.G. (2008) *A Description of the Advanced Research WRF Version 3*, NCAR Technical Note, USA, 88p.

Taha, H. (1997) Urban climates and heat islands: albedo, evapotranspiration, and anthropogenic heat. *Energy Build.* **25**(2), 99–103, doi: 10.1016/S0378-7788(96)00999-1

Tursilowati, L., Adiningsih, E.S., Sumantyo, J.T.S. & Kuze, H. (2009) Impact of land cover change to climate scenario by using remote sensing data and the weather research forecasting (WRF) model. *Proc. 47th Autums Conference of The Remote Sensing Society of Japan*, 63–64.

UCAR (University Corporation for Atmospheric Research). (2010) NCEP FNL Operational Model Global Tropospheric Analyses, continuing from July 1999. Available in: http://dss.ucar.edu/datasets/ds083.2. Accessed in 12 February 2010.

Wang, W., Barker, D., Bray, J., Bruyere, C., Duda, M., Dudhia, J., Gill, D. & Michalakes, J. (2007) ARW (Advanced Research of Weather Research & Forecasting) version 2, Modeling System User's Guide. Mesoscale & Microscale Meteorology Division, National Center for Atmospheric Research. Available in: http://www.mmm.ucar.edu/wrf/users.

WRF Model Website (2010) About the Weather Research & Forecasting Model. Available in http://www.wrf-model.org/index.php. Accessed in 16 October 2010.